

THE CREEP OF ICE SHELVES: INTERPRETATION OF OBSERVED BEHAVIOUR

By R. H. THOMAS

(British Antarctic Survey, Scott Polar Research Institute, Cambridge, England)

ABSTRACT. Available measurements of creep rates and dimensions of ice shelves are used, in conjunction with equations derived in a companion paper (Thomas, 1973), to evaluate the flow law parameters B and n for stresses down to 10^4 N m^{-2} . The results show good agreement with laboratory work at higher stresses. Adoption of these values of B and n enables us to examine the restraining effects on an ice shelf of obstructions such as areas of grounding.

RÉSUMÉ. Le fluage des plateformes de glace: interprétation des comportements observés. Les mesures disponibles sur la taille et la vitesse de fluage des plateformes de glace sont utilisées conjointement avec les équations établies dans un article voisin (Thomas, 1973) pour estimer la valeur des paramètres B et n de la loi d'écoulement pour des contraintes descendant jusqu'à 10^4 N m^{-2} . Les résultats sont en bon accord avec des travaux de laboratoire sous des contraintes supérieures. L'adoption de ces valeurs pour B et n nous met en mesure d'examiner l'effet freineur, sur une plateforme de glace, d'obstacles tels qu'une aire dans laquelle la plateforme touche le socle rocheux.

ZUSAMMENFASSUNG. Das Kriechen von Schelfeisen: Interpretation beobachteten Verhaltens. Verfügbare Messungen der Kriechgeschwindigkeit und der Ausdehnung eines Schelfeises werden in Verbindung mit Gleichungen aus einem gleichzeitig erscheinenden Aufsatz (Thomas, 1973) benutzt, um die Parameter B und n des Fließgesetzes für Spannungen bis herunter zu 10^4 N m^{-2} zu ermitteln. Die Ergebnisse zeigen gute Übereinstimmung mit Laborarbeiten bei höheren Spannungen. Die Annahme dieser Werte für B und n ermöglicht die Prüfung der nicht berücksichtigten Auswirkungen von Hindernissen auf ein Schelfeis, wie etwa in Gebieten mit Bodenkontakt.

HERE we shall use the expressions derived in another paper in this *Journal* (Thomas, 1973), together with measured values of creep rate from a number of ice shelves, to evaluate the parameters B and n in the flow law of ice. We shall consider separately the creep rates from relatively unconfined areas of ice shelf and those from a confined ice shelf—the Amery Ice Shelf. Finally we shall use the resultant values of B and n to interpret the behaviour of the Brunt Ice Shelf as it approaches a small ice rise.

First, however, we must note the influence of density variations with depth in equation (18) of Thomas (1973).

1. DEPTH/DENSITY FUNCTION

The flow law for ice can be written:

$$\dot{\gamma} = (\tau/B)^n \tag{1}$$

where the shear strain-rate $\dot{\gamma}$ is defined by

$$2\dot{\gamma}^2 = \dot{\epsilon}_{xx}^2 + \dot{\epsilon}_{yy}^2 + \dot{\epsilon}_{zz}^2 + 2\dot{\epsilon}_{xy}^2 + 2\dot{\epsilon}_{xz}^2 + 2\dot{\epsilon}_{yz}^2,$$

and for an ice shelf with $\dot{\epsilon}_{xz} = \dot{\epsilon}_{yz} = 0$, and using the notation of Thomas (1973),

$$\dot{\gamma} = +(1 + \alpha + \alpha^2 + \beta^2)^{\frac{1}{2}} |\dot{\epsilon}_{xx}|. \tag{2}$$

Also from equations (13) and (14) in Thomas (1973)

$$\tau = + \frac{(1 + \alpha + \alpha^2 + \beta^2)^{\frac{1}{2}}}{H|2 + \alpha|} \left| \int_b^s \int_z^s g\rho_1(z) dz dz - F \right|. \tag{3}$$

In order to simplify Equation (3) we might be tempted to assume the density of the ice shelf to be constant and equal to $\bar{\rho}_i$. With this assumption, however, values of τ are approximately double those obtained with a density/depth relationship similar to that found by Schytt (1958) at Maudheim.

Measurements of density versus depth were not made on the Brunt Ice Shelf, so we adopt a density function compatible with the observed relationship between ice thickness H and surface elevation h . To describe the Maudheim observations Schytt (1958, p. 120) suggested a function of the form:

$$\rho_i(z) = 917 \text{ kg m}^{-3} - k \exp[-\nu(h-z)] \quad (4)$$

where k and ν are empirical constants and z is measured upwards from sea-level.

Measurements of density near the surface give a value for $\rho_i(h)$ (we neglect the very low-density surface snow) so

$$k = 917 \text{ kg m}^{-3} - \rho_i(h).$$

For hydrostatic equilibrium we also have:

$$\begin{aligned} \int_b^s \rho_i(z) dz &= \rho_w(H-h) \\ &= (917 \text{ kg m}^{-3}) H + \frac{k \exp(-\nu H)}{\nu} - \frac{k}{\nu}. \end{aligned}$$

At Maudheim $\nu \approx 0.0258 \text{ m}^{-1}$ and $H \approx 200 \text{ m}$ (Schytt, 1958, p. 120) so $\exp(-\nu H) \ll 1$ and, assuming $\rho_w = 1028 \text{ kg m}^{-3}$,

$$\nu \approx k / [(1028 \text{ kg m}^{-3}) h - (111 \text{ kg m}^{-3}) H].$$

Thus we can evaluate ν wherever H and h are known. The "density function" (Equation (4)) together with the values of α and β from strain-rate measurements can then be substituted in Equation (3) to give τ .

We shall consider data from four ice shelves. For Maudheim we use the values of k and ν given by Schytt. For the Brunt Ice Shelf and the Amery Ice Shelf we adopt the Maudheim value of k (implying $\rho_i(h) = 450 \text{ kg m}^{-3}$) and deduce ν from local measurements of H and h (the Brunt Ice Shelf measurements are described in Thomas and Coslett (1970); those for the Amery Ice Shelf were from preliminary results communicated to the author by W. F. Budd in 1971). Evaluation of Equation (3) for "Little America V" on the Ross Ice Shelf was by numerical integration of the observed variation of density with depth (Crary, 1961, p. 42). Note that the results given by Thomas (1971) assumed that Equation (4) adequately represented density variation at "Little America". However, the observed density profile shows an increased rate of densification at about 40 m depth. Gow (1963, p. 278) believed this to be the remnant effects of horizontal compression near Roosevelt Island. In these circumstances Equation (4) leads to an over-estimated value of τ . A similar situation probably exists on the Brunt Ice Shelf with compressive strain-rates up-stream from the McDonald Ice Rumples (Fig. 4).

2. UNBOUNDED ICE SHELF

With $\beta = 0$ in Equation (2) and $F = \frac{1}{2} \rho_w (H-h)^2$ in Equation (3) we have equations which apply to areas of ice shelf confined in the x -direction solely by sea pressure. $\dot{\epsilon}_{xx}$ and $\dot{\epsilon}_{yy}$ are then the principal components of the horizontal strain-rate, and from equation (16) in Thomas (1973) we see that the strain-rate reaches a maximum in the x -direction where F is a minimum. Thus we take $\dot{\epsilon}_{xx}$ as the larger principal component of the horizontal strain-rate.

In Table I values of H , h , ν , $\dot{\epsilon}_{xx}$, α , $\dot{\gamma}$, and τ are listed for a number of apparently unconfined areas of ice shelf. Because the Amery Ice Shelf is bounded, only data from G1, situated nearer the ice front than the ice-shelf sides, has been used. G1 is situated on a small hill rising some 10 m above the surrounding ice shelf and two values of τ have been calculated corresponding to local and regional values of H and h . The Brunt Ice Shelf data were selected from areas apparently free from horizontal shear or compressive strains.

TABLE 1. CALCULATION OF EFFECTIVE STRAIN-RATES AND STRESS FOR UNBOUNDED ICE SHELVES

Strain figure	$10^4 \dot{\epsilon}_x$ a ⁻¹	α	$10^{12} \dot{\gamma}$ s ⁻¹	h m	H m	ν m ⁻¹	$10^{-6} \int_b^s \int_z^s \rho(z) dz dz$	$\frac{1}{2} \rho_w (H-h)^2 \times 10^{-6}$ kg m ⁻¹	τ MN m ⁻²	B MN m ⁻² s ^{1/3}
							kg m ⁻¹			
R1*	4.9	0.88	25	27	150	0.042	8.913	7.776	0.042	144
R2*	8.1	0.89	42	30	180	0.043	13.153	11.565	0.049	141
31 32 33*	14.1	0.43	57	35.5	245	0.050	25.420	22.560	0.060	156
24 25 26 27*	6.5	0.23	23	26.5	185	0.070	14.553	12.913	0.044	155
27 28 29*	9.3	0.30	35	29	215	0.079	19.998	17.782	0.052	159
37 38 39*	18.3	0.03	59	36.5	255	0.051	27.659	24.540	0.060	154
38 39 41*	22.7	0.03	73	37	260	0.051	28.793	25.561	0.061	146
Little America	12.9	0.63	58	43	257	—	26.524	23.539	0.062	160
Maudheim	13.8	0.40	55	37	190	0.026	13.830	12.032	0.048	126
Local										
G1 (Amery)	60	0.13	204	64	425	0.025	75.625	66.032	0.100	169
Regional										
G1 (Amery)	60	0.13	204	53	380	0.038	61.861	54.962	0.090	153
R7*	11	-1.41	44	7.0	28	—	0.273	0.232	0.030	85
Ward Hunt	1.2	-0.5	3.3	4.4	37	—	0.623	0.546	0.012	77

See Thomas (1973) and section 1 for explanation of symbols used

Values of τ for R7, "Little America", and Ward Hunt Ice Shelf were obtained by integrating the observed depth/density curves.

The sources of data used are:

- Amery Ice Shelf: Budd (1966) and personal communication from W. F. Budd in 1971;
- "Little America": Crary (1961);
- Maudheim: Swithinbank (1958), Schytt (1958) and Crary (1961, p. 100);
- Ward Hunt Ice Shelf: Dorrer (1971).

* Brunt Ice Shelf data. The numbers refer to movement stakes shown in Figure 4.

From Equation (1) we have:

$$\log \dot{\gamma} = n \log (\tau/\bar{B}).$$

So, for an almost constant \bar{B} , we plot $\log \dot{\gamma}$ against $\log \tau$ to obtain a straight line of slope n (Fig. 1). The line represented by $n = 3$ fits the data well, implying a behaviour consistent with Walker's (unpublished) laboratory results at stresses down to 0.04 MN m⁻². The lower stress region of Walker's results for -14° C and -22° C is included in Figure 1 for comparison. Most of the scatter of the ice-shelf results can be attributed to differences between the mean temperatures (and hence the values of \bar{B}) of the various ice shelves. With $n = 3$ in Equation (1) we can calculate values of B for each of the four ice shelves; the results are listed in Table I and plotted against mean ice-shelf temperature in Fig. 2. The temperature measurements used are from Schytt (1960, p. 167), Crary (1961, p. 56) and a personal communication from W. F. Budd in 1970. The temperature/depth variation for Brunt Ice Shelf is assumed to be similar to that at Maudheim.

Also shown in Figure 2 is a $B-T$ graph deduced from Walker's (unpublished, table 3, "power law region") laboratory results, and theoretical values of \bar{B} calculated for each ice shelf using this graph and the known, or assumed, variation of temperature with depth. Because of the non-linear form of the $B-T$ curve the creep behaviour of the ice shelf is determined more by the colder ice and this is reflected in the small difference between mean ice-shelf temperatures and those against which theoretical values of \bar{B} have been plotted in Figure 2. However, in calculating the mean ice-shelf temperatures and theoretical values of \bar{B} , temperatures in the upper 40 m of low density, relatively soft firn have been neglected.

Although Figure 2 shows good agreement between field results and laboratory work, it is significant that the field values of \bar{B} are each slightly larger than expected and the ice shelves appear harder than laboratory ice at the same temperature. If, as discussed earlier, the

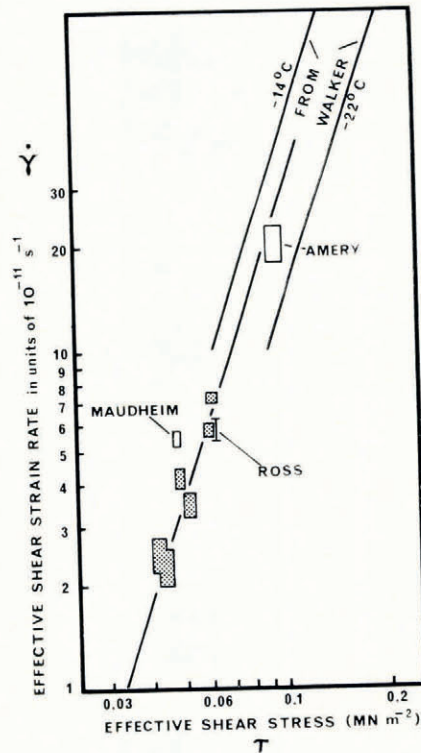


Fig. 1. Log-log plots of effective shear strain-rate against effective shear stress for ice shelves of differing thickness. The unlabelled points are from the Brunt Ice Shelf. Laboratory results from Walker (unpublished) are included. The error rectangles incorporate errors in strain rate, surface elevation and ice thickness. No allowance is made for errors in the form of the assumed depth/density curve.

density/depth curve for the Brunt Ice Shelf is similar to that found at "Little America V" the values of τ and \dot{B} found using Equation (4) will be too high. Thus only the value of \dot{B} from G1 on the Amery Ice Shelf is significantly different from that deduced from laboratory results. This is believed to be because the ice at G1 is to a certain extent restrained by the ice-shelf sides so that its behaviour is more accurately described by the analysis given in section 3.2 of Thomas (1973). In section 3 we shall use measurements of the dimensions of the Amery Ice Shelf (personal communication from W. F. Budd in 1971 of thicknesses from radio echo sounding and surface elevations from precision levelling) to interpret strain-rates measured on the ice shelf. First, however, we shall use data collected on thin ice shelves to extend our knowledge of the flow law to lower stresses.

2.1. Results from areas of thin ice shelf

In a recent paper Dorrer (1971) presented measurements of ice velocity and strain-rates from the Ward Hunt Ice Shelf taken at a point where the ice is approximately 40 m thick. The values are shown in Figure 3 (a reproduction of Dorrer's figure 4). Dorrer deduced values of n and \dot{B} from these results, but his analysis utilised Nye's (1952) solution for the velocity in an infinitely deep channel (which assumes zero longitudinal strain-rate) and Budd's (1966) expression for \dot{B} (which is only valid for an ice shelf of uniform thickness).

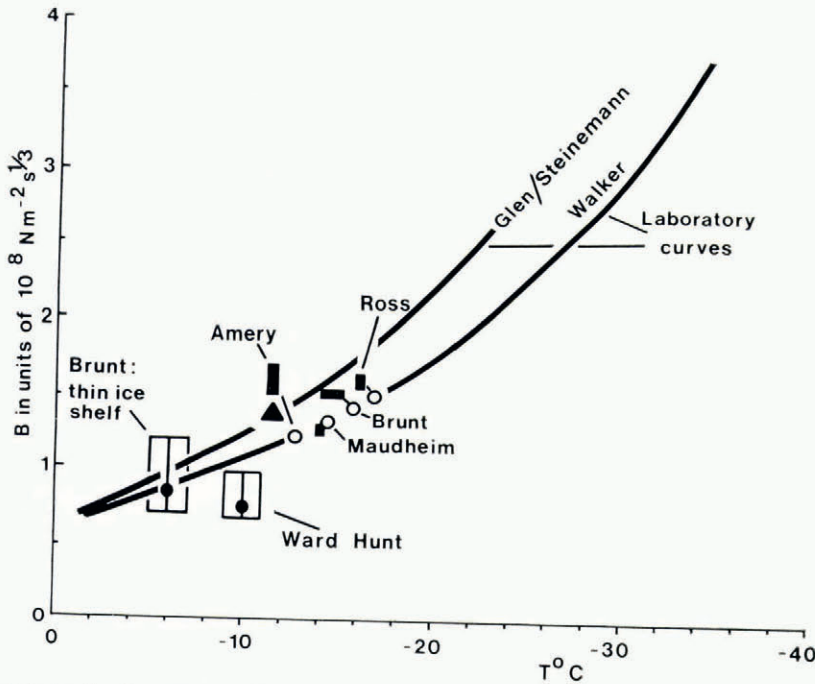


Fig. 2. Plot of the ice flow-law parameter B against temperature. Ice-shelf values of B averaged over depth (■) assuming unconfined "Weertman" creep are compared with those (○) deduced from the B - T curve based on Walker's (unpublished) laboratory results. Correction for the restraining effects of the ice-shelf sides gives a reduced value of \bar{B} (▲) for the Amery Ice Shelf.

The ice velocities in the neighbourhood of the strain network are so small ($\approx 0.5 \text{ m a}^{-1}$) that the effects of shear stresses between the grounded and floating ice are likely to be negligible. Consequently we shall consider that stresses in the direction of ice movement (the x -direction) are balanced solely by sea pressure.

We adopt a similar approach to strain-rates measured at R7 on a thin area of the Brunt Ice Shelf (Figs. 4 and 5) with x -direction parallel to the larger component of strain-rate. $\dot{\gamma}$ and τ were calculated using Equations (2) and (3).

$$\int_b^s \int_z^s \rho_i(z) dz dz$$

was calculated for R7 by numerical integration of the observed variation of density with depth, and for the Ward Hunt Ice Shelf by assuming a constant density of 910 kg m^{-3} . The results are included in Table I and plotted as $\log \tau$ versus $\log \dot{\gamma}$ in Figure 6. The 10 m temperature at R7 is -10° C and on the Ward Hunt Ice Shelf (Lyons and Ragle, 1962) the surface temperature is approximately -18° C . Assuming a linear increase of temperature with depth to -2° C at the base we estimate equivalent average temperatures of -6° C and -10° C . Included in Figure 6 are the plots of $\log \tau$ versus $\log \dot{\gamma}$ appropriate to these temperatures assuming the laboratory B - T curve and a flow-law exponent of $n = 3$. The error boxes drawn around the field values include the effects solely of strain-rate errors, so the field results show a satisfactory agreement with the extrapolated laboratory results for stresses down to $1 \times 10^4 \text{ N m}^{-2}$.

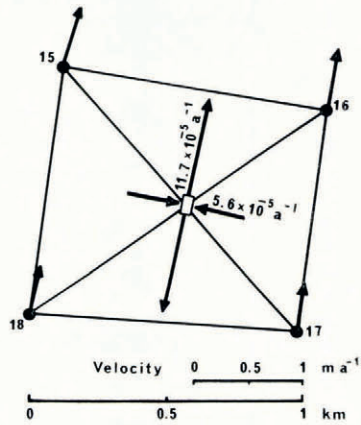


Fig. 3. Velocity vectors and principal strain-rates at a strain network on the Ward Hunt Ice Shelf. From Dorrer (1971).

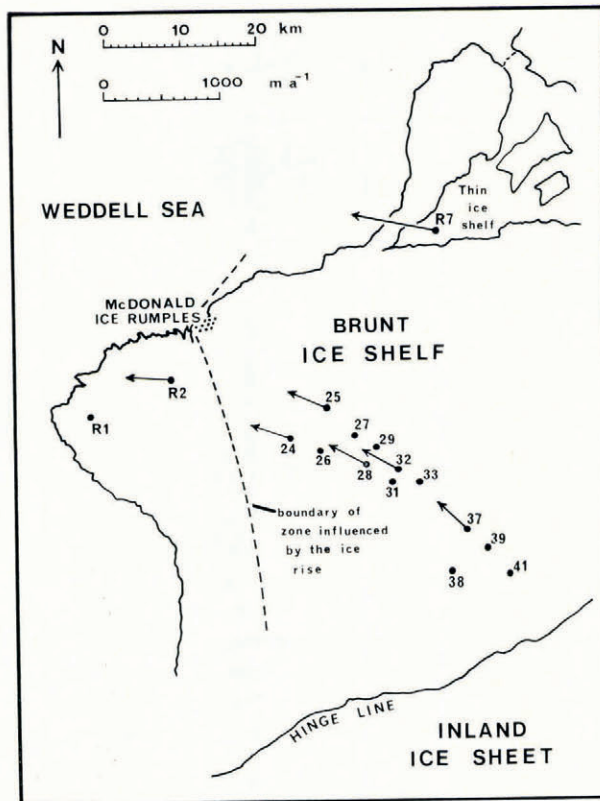


Fig. 4. The western part of Brunt Ice Shelf showing a selection of movement markers and velocity vectors.

This is shown by Figure 2, where values of \dot{B} for the areas of thin ice shelf (obtained by substituting τ and $\dot{\gamma}$ in Equation (1)) are plotted against temperature. However, in contrast to most of the thicker ice shelves studied, the areas of thin ice shelf appear if anything slightly softer than expected. One reason for this could be the relatively high impurity levels: the Ward Hunt Ice Shelf contains an appreciable percentage of old sea ice (Lyons and Ragle, 1962) and movement studies near R7 (Fig. 5) indicate that in 1967 the thin ice shelf was

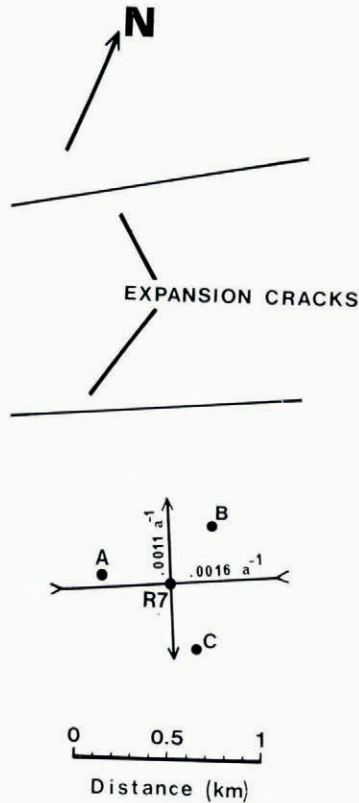


Fig. 5. Strain-rates measured on a thin area of Brunt Ice Shelf.

probably less than 20 years old and consisted largely of old sea ice with a surface cover of firn and snow. However, we should also note that on both the areas of thin ice shelf the total strain suffered by the ice is probably less than 10% and steady state may not have been reached (Weertman, 1969). In either case we expect true steady-state strain-rates to be lower than those shown in Figure 6.* This would probably lead to better agreement with the extrapolated laboratory results implying no reduction in n down to effective stresses of 10^4 N m^{-2} .

* Personal communication from G. Holdsworth in 1972 indicates that the Ward Hunt Ice Shelf may be grounded over a larger area than previously supposed. If the grounding is found to extend beneath the site of Dorrer's survey then the above analysis cannot be applied to his results.

The very close agreement between the value of \bar{B} from R7 and that for laboratory ice at the same temperature implies that in this instance the ice shelf behaves almost as pure ice. This may be indicative of the extent to which sea ice can be desalinated.

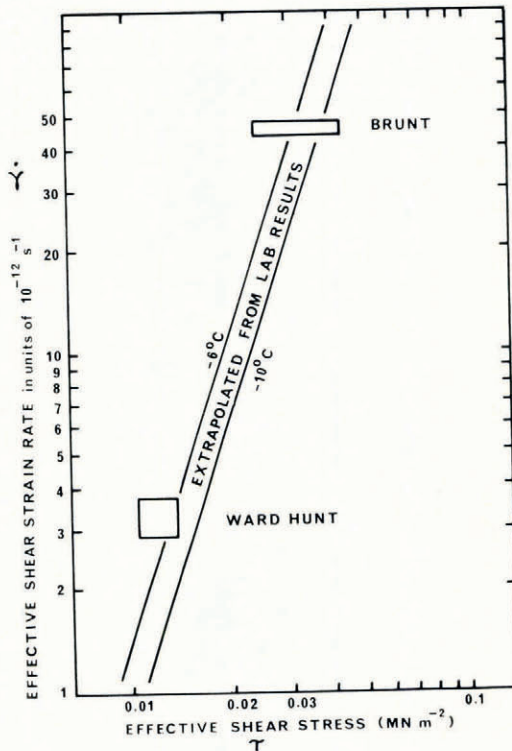


Fig. 6. Log-log plot of effective shear strain-rate against effective shear stress for areas of thin ice shelf. Extrapolated curves from Walker's (unpublished) laboratory results are included.

3. CREEP RATES ON THE AMERY ICE SHELF

The Amery Ice Shelf is shown in Figure 7. Strain-rates at G1, G2, G3 and E are given in Budd (1966) and Budd and others (1967). Of these four stations only E is sufficiently far from the centre line to supply measurements of the shear strain-rate $\dot{\epsilon}_{xy}$ necessary for the solution of equation (29) in Thomas (1973) to give \bar{B}

$$\bar{B} = \frac{(1 + \alpha + \alpha^2 + \beta^2)^{(n-1)/2n} \rho_1 g h}{2 |\dot{\epsilon}_{xx}|^{1/n} \left\{ \frac{|\dot{\epsilon}_{xx}|}{\dot{\epsilon}_{xx}} (2 + \alpha) + \frac{|\beta| a}{yH} \int_x^X \frac{H dx}{a} \right\}} \quad (5)$$

All calculations incorporate variation of density with depth as described in section 1.

Before solving this, however, we must elaborate our definition of the line across the ice shelf defined by $x = X$ and beyond which the sides of the ice shelf no longer affect creep behaviour. In section 2 we assumed that G1 is to seaward of this line because it is sited nearer the ice front than the ice-shelf sides. However, the resultant value of \bar{B} showed that this is probably not true. Here we assume that $x = X$ describes a quasi-circular arc through the points where the ice shelf leaves its margins and inclined at 45° to the margins at these points (Fig. 7).

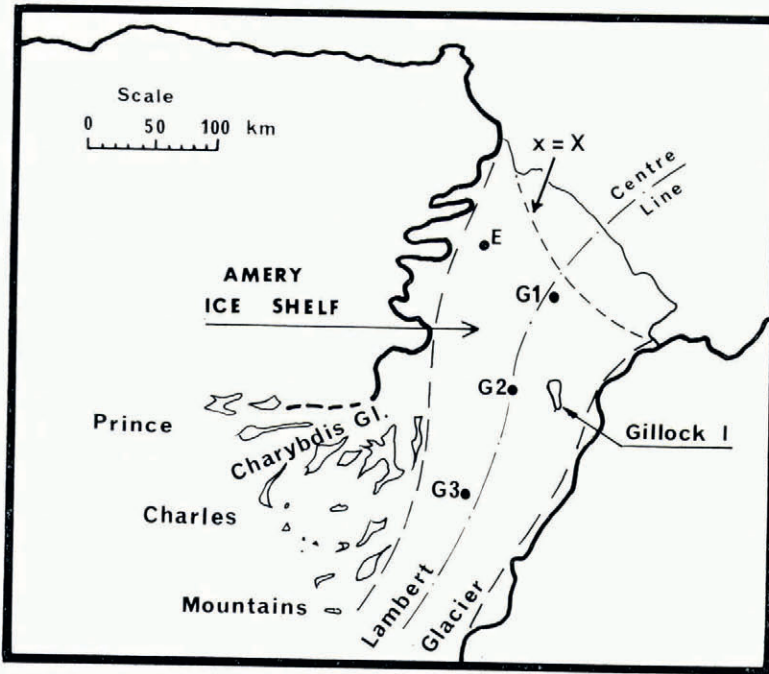


Fig. 7. Plan view of the Amery Ice Shelf showing positions of strain networks. From Budd (1966) with modifications.

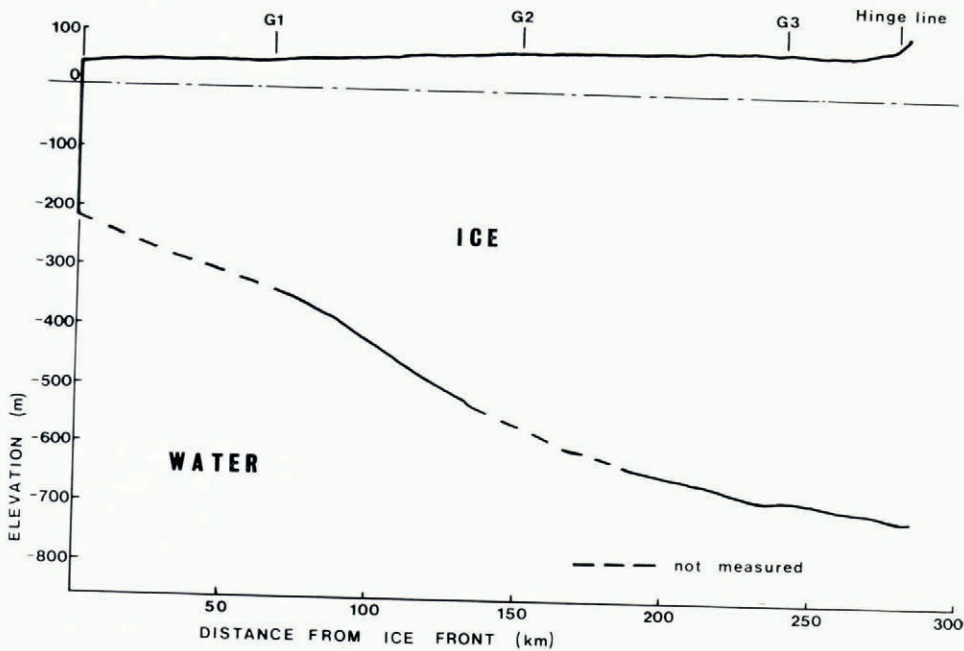


Fig. 8. Vertical section of the Amery Ice Shelf taken along the centre line. Personal communication from Budd.

There are no measurements available for ice thickness and surface elevation from the ice front to E so we assume a similar profile to that measured along the centre line (Fig. 8). The values of relevant parameters are given in Table II. Substituting these values in Equation (5) and assuming $n = 3$ we get

$$\bar{B} = 1.39 \times 10^8 \text{ N m}^{-2} \text{ s}^{\frac{1}{3}}$$

Using equation (26) of Thomas (1973) we can now evaluate $\bar{\tau}_s$, the shear stress at the ice-shelf sides averaged over thickness

$$\bar{\tau}_s = -9 \times 10^4 \text{ N m}^{-2}$$

which is approximately the value associated with a plastic "yield stress" for ice (see for instance Paterson, 1969, p. 88).

TABLE II. CALCULATION OF \bar{B} AND F_b AT VARIOUS POINTS ON THE AMERY ICE SHELF

Station	Distance from line $x = X$ km	h m	H m	$\int_x^X (H/a) dx$ m	ν	$10^{-6}A = 10^{-6} \int_b^s \int_z^s \rho(z) dz dz$		$10^{-6}A' = \frac{1}{2}\rho_w(H-h)^2 \times 10^{-6}$
						kg m ⁻¹	kg m ⁻¹	
G1 (local)	15	64	425	75	0.025	75.625	61.861	66.985
G1 (regional)	15	53	380	75	0.038	61.861	—	54.962
G2	95	76	625	650	0.053	178.761	—	154.920
G3	195	85	750	1980	0.113	254.843	—	227.304
E	45	53	380	190	0.038	61.861	—	54.962

Station	$g(A-A')/H$ MN m ⁻²	a km	y km	$10^4 \epsilon_{xx}$ a ⁻¹	$10^{12} \epsilon_{xx}$ s ⁻¹	α	β	B MN m ⁻² s ^{1/3}	F_b MN m ⁻¹
G1 (local)	0.199	80	10	60	190	0.13	0	157	0
G1 (regional)	0.178	80	10	60	190	0.13	0	137	0
G2	0.296	53	15	17	54	0.03	0	—	60
G3	0.360	43	10	5	16	0.30	0	—	40
E	0.178	80	60	70	222	0	1	139	0

See Thomas (1973) and sections 1 and 3 for explanation of the symbols used

We are now in a position to calculate an improved value of \bar{B} from the data obtained at G1. For positive ϵ_{xx} , equation (23) of Thomas (1973) can be written:

$$\bar{B} = \left\{ \frac{\rho_1 g h}{2} + \frac{\bar{\tau}_s}{H} \int_x^X \frac{H dx}{a} \right\} / \left\{ \frac{\epsilon_{xx}}{\theta} \right\}^{1/n} \tag{6}$$

with

$$\theta = (1 + \alpha + \alpha^2 + \beta^2)^{(n-1)/2} / |2 + \alpha|^n$$

Using the values listed in Table II we get

$$\bar{B} = 1.37 \times 10^8 \text{ N m}^{-2} \text{ s}^{\frac{1}{3}}$$

if we use the regional rather than local values of surface elevation and ice thickness. This is almost identical to the value deduced from observations at E. Errors are difficult to assess, being largely due to possible deviations of the actual depth/density function from that represented by Equation (4). However, these values compare well with that deduced for ice at G1 ($1.25 \times 10^8 \text{ N m}^{-2} \text{ s}^{\frac{1}{3}}$) from the laboratory B - T curve.

At greater distances from the ice front the strain-rates are considerably reduced and they become comparable with the estimated errors. Moreover near G2 there is probably a "bottle-neck" effect due to the presence of Gillock Island and to the large influx of ice from Charybdis Glacier (Fig. 7). This should cause a local increase in the up-stream restraining force F which

becomes the sum of the forces due to water pressure F_w , shear past the sides F_s and "bottle-neck" restraint F_b . Equation (16) of Thomas (1973) then becomes:

$$\dot{\epsilon}_{xx} = \theta \left\{ \frac{\rho_1 g h}{2B} - \frac{(F_s + F_b)}{HB} \right\}^n, \tag{7}$$

or, using equation (22) of Thomas (1973) and generalizing for negative $\dot{\epsilon}_{xx}$

$$F_b = \frac{\rho_1 g h H}{2} + \bar{\tau}_s \int_x^x \frac{H dx}{a} - \frac{\dot{\epsilon}_{xx}}{|\dot{\epsilon}_{xx}|} (2 + \alpha) HB \left\{ \frac{|\dot{\epsilon}_{xx}|}{(1 + \alpha + \alpha^2 + \beta^2)^{(n-1)/2}} \right\}^{1/n}. \tag{8}$$

Substituting the values listed in Table II and assuming $B \sim 1.4 \times 10^8 \text{ N m}^{-2} \text{ s}^{\frac{1}{2}}$ we get:

$$\left. \begin{aligned} \text{At G1 } F_b &= 0 \\ \text{At G2 } F_b &= 6 \times 10^7 \\ \text{At G3 } F_b &= 4 \times 10^7 \end{aligned} \right\} \text{Newtons per metre width of ice shelf.}$$

The errors in strain-rate are such that the values of F_b at G2 and G3 are effectively equal. This means that the creep behaviour of the ice shelf up-stream of G2 can be interpreted by Equations (5) and (6) if we incorporate an additional constraint F_b which is approximately constant at all points, and is probably due to the presence of Gillock Island and Charybdis Glacier. A more detailed analysis would require data from a larger number of stations and in the next section we shall use the results of the survey work on the Brunt Ice Shelf described in Thomas (1970) to examine the influence of a small ice rise (McDonald Ice Rumples in Fig. 4) on the creep behaviour of the Brunt Ice Shelf.

4. THE INFLUENCE OF THE McDONALD ICE RUMPLES ON THE BRUNT ICE SHELF

The effect of a small ice rise on a moving ice shelf is analogous to that of a large restraining force acting at the centre of the ice rise. Because the ice is floating, this force will be largely transmitted up-stream through a zone of disturbed ice where strain-rates are affected by the ice rise. Within this zone we expect an inverse relationship between distance r from the ice rise and the local value of the restraining force $F(r)$ per unit width of ice shelf. More specifically we can write

$$F(r) \propto 1/r^m. \tag{9}$$

In this section, by examination of the observed variation of $F(r)$ with r , we shall deduce an approximate shape for the disturbed zone and calculate the stresses acting within the area of grounded ice.

4.1. The restraining force exerted on the ice shelf by the McDonald Ice Rumples

For the strain-rates measured on the Brunt Ice Shelf up-stream from the McDonald Ice Rumples Equation (8) becomes

$$F(r) = \frac{\rho_1 g h H}{2} - \frac{\dot{\epsilon}_{xx}}{|\dot{\epsilon}_{xx}|} (2 + \alpha) HB \left\{ \frac{|\dot{\epsilon}_{xx}|}{(1 + \alpha + \alpha^2 + \beta^2)^{(n-1)/2}} \right\}^{1/n} \tag{10}$$

where $F(r)$ is the restraining force exerted by the McDonald Ice Rumples on a unit width of the ice shelf at the point where $\dot{\epsilon}_{xx}$ is measured and x is the direction from that point towards the McDonald Ice Rumples.

Principal strain-rates ($\dot{\epsilon}_1$ and $\dot{\epsilon}_2$) resulting from the ice velocity measurements described in Thomas (1970) were converted to their components in the x , y and xy directions using:

$$\begin{aligned}\dot{\epsilon}_{xx} &= \frac{1}{2}(\dot{\epsilon}_1 + \dot{\epsilon}_2) + \frac{1}{2}(\dot{\epsilon}_1 - \dot{\epsilon}_2) \cos 2\theta, \\ \dot{\epsilon}_{yy} &= \frac{1}{2}(\dot{\epsilon}_1 + \dot{\epsilon}_2) - \frac{1}{2}(\dot{\epsilon}_1 - \dot{\epsilon}_2) \cos 2\theta, \\ \dot{\epsilon}_{xy} &= \frac{1}{2}(\dot{\epsilon}_1 - \dot{\epsilon}_2) \sin 2\theta,\end{aligned}$$

where θ is the angle between the directions of $\dot{\epsilon}_{xx}$ and $\dot{\epsilon}_1$. Assuming $n = 3$ and $B \approx 1.5 \times 10^8 \text{ N m}^{-2} \text{ s}^{\frac{1}{3}}$ and taking appropriate values of h and H from the surface elevation and ice thickness measurements, Equation (10) was solved for numerous points within the area of ice shelf influenced by the McDonald Ice Rumples. The results are plotted as $\log F(r)$ versus $\log r$ in Figure 9.

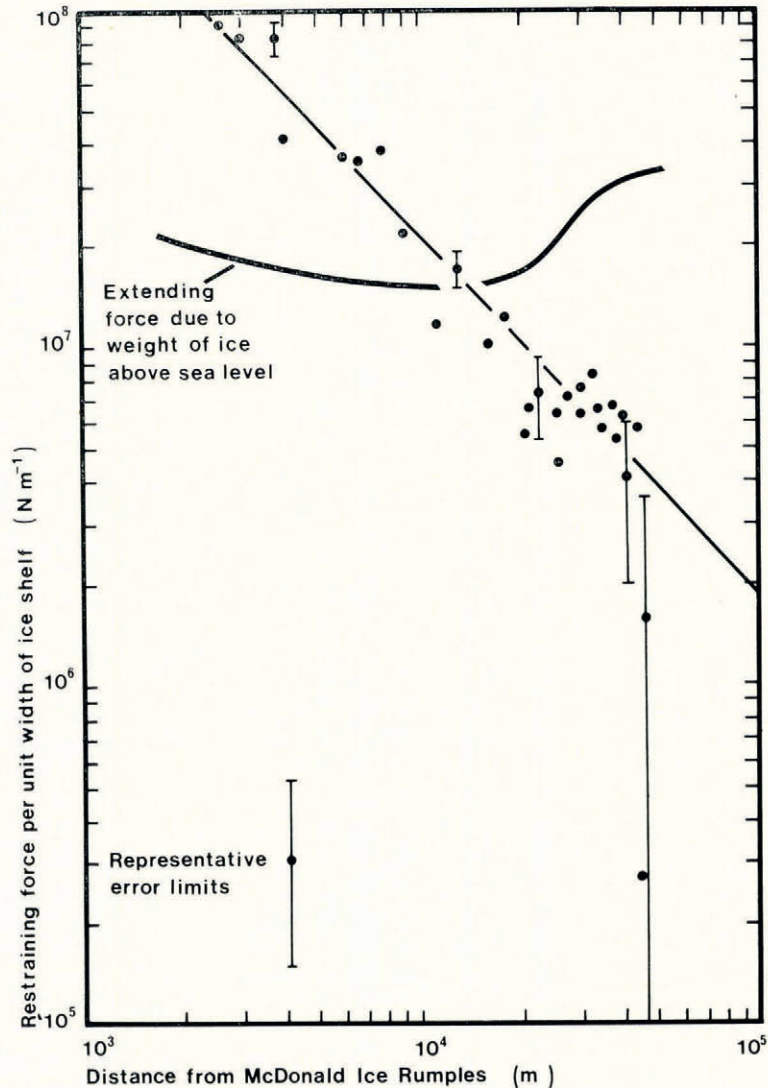


Fig. 9. Restraining force exerted by the McDonald Ice Rumples plotted against distance from the ice rise.

In order to give an idea of the relative magnitudes involved, a plot of horizontal tensile force due to the weight of ice above sea-level ($= \frac{1}{2}\rho_i g h H$) is included. Division by the ice thickness gives the appropriate average stresses. The rapid decrease in $F(r)$ at $r \sim 40$ km is associated with entry into an area of ice shelf that consists of a matrix of loosely consolidated icebergs.

4.2. *The shape of the disturbed zone*

Observations on the Brunt Ice Shelf indicate that there is a discrete zone up-stream of the McDonald Ice Rumples where strain-rates are influenced by the restraining effects of the grounded ice. The first-order regression line of slope -1.07 is included in Figure 9. The degree of agreement between this line and the data points indicates that, for a given value of r , $F(r)$ is more or less independent of position within the disturbed zone. However, this condition must break down near the margins of the zone, where $F(r)$ decreases to zero.

Because the ice shelf is floating the total force acting at any distance r from the ice rise is constant

$$F(r) r \phi(r) = \text{constant} \tag{11}$$

where $\phi(r)$ is the angle subtended at the ice rise by the disturbed zone at distance r . From the results illustrated in Figure 9 we also have

$$F(r) \approx \text{constant}/r^m$$

so we can write Equation (11) as

$$\phi(r) = k r^{m-1} \tag{12}$$

where k is some constant. We thus have the result that when $m = 1$, ϕ is independent of r . This corresponds to the case of a perfectly rigid body. In our case $m \approx 1.07$, implying a more rapid stress diffusion as a result of creep deformation. From a study of the strain-rate distribution near the McDonald Ice Rumples the value of ϕ corresponding to $r = 7$ km was estimated to be between 100° and 120° (≈ 2 rad). Thus k in Equation (12) is given by

$$k \approx \frac{2}{(7000)^{0.07}} \approx 1.1 \text{ rad m}^{-0.07}.$$

Substitution of this value into Equation (12) gives the boundaries to the zone of disturbance shown in Figure 4.

4.3. *Stresses at the ice rise*

The average stress $\bar{\sigma}$ acting across the boundary between the grounded ice of McDonald Ice Rumples and the ice shelf is H^{-1} times the value of $F(r)$ at r equal to the radius of the ice rise (≈ 0.5 km). Thus

$$\bar{\sigma} \approx \frac{5.2 \times 10^8}{3 \times 10^2} \approx 1.7 \times 10^6 \text{ N m}^{-2}$$

for $H = 300$ m. Figure 10 clearly illustrates the effects of these very large stresses on the ice shelf at the point of grounding.

The value of $F(r)$ corresponding to $r = 1/\phi(r)$ is equal to the total force F_t exerted by the ice shelf on the sea bed beneath the ice rise. Extrapolation of Figure 9 to this value of r (≈ 0.9 m) gives:

$$F_t \approx 4 \times 10^{11} \text{ N.}$$

This force is distributed over the area of ice actually grounded ($\approx 3.5 \text{ km}^2$). Thus we calculate a value for the basal shear stress τ_b :

$$\tau_b \approx \frac{4 \times 10^{11}}{3.5 \times 10^6} \approx 1.1 \times 10^5 \text{ N m}^{-2}$$

which is in good agreement with the plastic "yield stress" for ice.

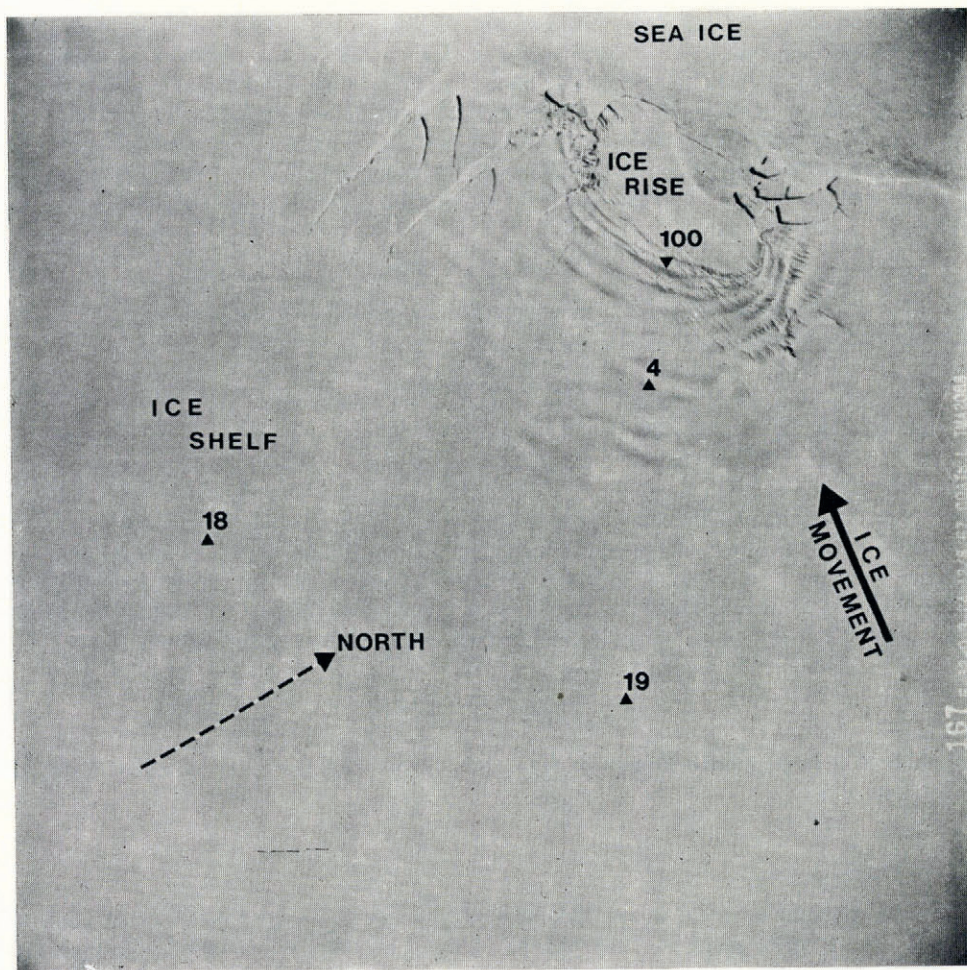


Fig. 10. Air photograph taken from 8 000 m above the McDonald Ice Rumples. December 1967.

5. CONCLUSIONS

Because of the very low strain-rates involved, laboratory experiments on the creep of ice become both time-consuming and unreliable at stresses much below 10^5 N m^{-2} . This is particularly so at temperatures less than -10° C where, for instance, a uniaxial stress of $5 \times 10^4 \text{ N m}^{-2}$ produces a strain-rate of less than $1 \times 10^{-3} \text{ a}^{-1}$. It is in this stress region that field glaciology is likely to supply more information.

Ice shelves rest on a frictionless bed of known temperature and their creep behaviour is relatively simple to analyse in terms of the generalized ice flow law $\dot{\gamma} = (\tau/B)^n$. They are therefore the natural ice features most likely to extend our knowledge of the flow-law parameters into the low-stress region.

In this paper we have used all published creep rates from ice shelves of known dimensions to compare field values of B and n with those deduced from laboratory work at stresses greater than $1 \times 10^5 \text{ N m}^{-2}$. The degree of agreement suggests that the generalized flow law can be applied with $n \approx 3$ at least over the stress range $1 \text{ MN m}^{-2} > \tau > 0.04 \text{ MN m}^{-2}$ and probably to stresses as low as 0.01 MN m^{-2} .

Results from thicker ice shelves show the ice to be slightly harder than Walker's laboratory ice at the same temperature. To a certain extent we expect this, since some of the driving force assumed to be responsible for creep may be otherwise employed. Other possible explanations include preferred fabric within ice shelves (discussed by Thomas, 1971) and grain-size effects. Little or no reliable work has been published on the effects of grain size on the creep properties of ice, but for polycrystalline metals the dependence of creep rate on grain size has been investigated to a greater extent. Sherby and Burke (1968, p. 353) suggest that in the power-law stress region grain size is of minor importance and at lower stresses the creep rate is unaffected at grain sizes above a critical value. Below this value creep rate increases with decreasing grain size. Work reviewed by Garofalo (1965, p. 28) shows that for monel and for an iron alloy there appears to be a critical value d_m of the grain diameter at which the secondary creep rate is a minimum. Values of d_m are almost independent of stress, but increase with rising temperature.

The separate experiments of Glen, Steinemann, and Walker each involved samples of approximately 1 mm grain diameter, which is appreciably smaller than the mean values at Maudheim and "Little America" (Gow, 1963, p. 281) where the grain diameter increases from 2 mm near the surface to about 7 mm at a depth of 150 m. Values of B for $n = 3$ derived from the results of Glen and Steinemann (after Budd, 1966, p. 351) are included in Figure 2. Despite the large differences in grain size the ice shelf results lie between the B versus T graph of Glen and Steinemann and that of Walker. This may imply either that grain size has little effect on the creep behaviour of ice, or that d_m falls between 1 mm and 7 mm in the temperature range -12°C and -18°C . However, considerably more laboratory data are required before any firm conclusions can be reached.

ACKNOWLEDGEMENTS

I thank the British Antarctic Survey for sponsoring this work, Dr W. F. Budd for supplying the Amery Ice Shelf data and members of the Scott Polar Research Institute for reading the manuscript. An anonymous referee brought to my notice the reference to Sherby and Burke (1968).

MS. received 5 February 1972 and in revised form 31 August 1972

REFERENCES

- Budd, W. F. 1966. The dynamics of the Amery Ice Shelf. *Journal of Glaciology*, Vol. 5, No. 45, p. 335-58.
 Budd, W. F., and others. 1967. The Amery Ice Shelf, by W. [F.] Budd, I. [H.] Landon-Smith and E. [R.] Wishart. (In Oura, H., ed. *Physics of snow and ice: international conference on low temperature science. . . . 1966. . . . Proceedings*, Vol. 1, Pt. 1. [Sapporo], Institute of Low Temperature Science, Hokkaido University, p. 447-67.)
 Crary, A. P. 1961. Glaciological studies at Little America station, Antarctica, 1957 and 1958. *IGY Glaciological Report Series* (New York), No. 5.
 Dorrer, E. 1971. Movement of the Ward Hunt Ice Shelf, Ellesmere Island, N.W.T., Canada. *Journal of Glaciology*, Vol. 10, No. 59, p. 211-25.
 Garofalo, F. 1965. *Fundamentals of creep and creep-rupture in metals*. New York, Macmillan.

- Gow, A. J. 1963. The inner structure of the Ross Ice Shelf at Little America V, Antarctica, as revealed by deep core drilling. *Union Géodésique et Géophysique Internationale. Association Internationale d'Hydrologie Scientifique. Assemblée générale de Berkeley, 19-8-31-8 1963. Commission des Neiges et des Glaces*, p. 272-84.
- Lyons, J. B., and Ragle, R. H. 1962. Thermal history and growth of the Ward Hunt Ice Shelf. *Union Géodésique et Géophysique Internationale. Association Internationale d'Hydrologie Scientifique. Commission des Neiges et des Glaces. Colloque d'Obergurgl, 10-9-18-9 1962*, p. 88-97.
- Nye, J. F. 1952. The mechanics of glacier flow. *Journal of Glaciology*, Vol. 2, No. 12, p. 82-93.
- Paterson, W. S. B. 1969. *The physics of glaciers*. Oxford, etc., Pergamon Press. (The Commonwealth and International Library. Geophysics Division.)
- Schytt, V. 1958. Glaciology. II. The inner structure of the ice shelf at Maudheim as shown by core drilling. *Norwegian-British-Swedish Antarctic Expedition, 1949-52. Scientific Results*, Vol. 4, C.
- Schytt, V. 1960. Glaciology. II. Snow and ice temperatures in Dronning Maud Land. *Norwegian-British-Swedish Antarctic Expedition, 1949-52. Scientific Results*, Vol. 4, D.
- Sherby, O. D., and Burke, P. M. 1968. Mechanical behaviour of crystalline solids at elevated temperature. *Progress in Materials Science*, Vol. 13, p. 325-90.
- Swithinbank, C. W. M. 1958. Glaciology. I. The movement of the ice shelf at Maudheim. *Norwegian-British-Swedish Antarctic Expedition, 1949-52. Scientific Results*, Vol. 3, C.
- Thomas, R. H. 1970. Survey on moving ice: a sixty kilometres long triangulation net across an Antarctic ice shelf. *Survey Review*, Vol. 20, No. 157, p. 322-38.
- Thomas, R. H. 1971. Flow law for Antarctic ice shelves. *Nature, Physical Science*, Vol. 232, No. 30, p. 85-87.
- Thomas, R. H. 1973. The creep of ice shelves: theory. *Journal of Glaciology*, Vol. 12, No. 64, p. 45-53.
- Thomas, R. H., and Coslett, P. H. 1970. Bottom melting of ice shelves and the mass balance of Antarctica. *Nature*, Vol. 228, No. 5266, p. 47-49.
- Walker, J. C. F. Unpublished. The mechanical properties of ice Ih. [Ph.D. thesis, University of Cambridge, 1970. For a published account of much of this work, see Barnes, P., and others. 1971. Friction and creep of polycrystalline ice, by P. Barnes, D. Tabor and J. C. F. Walker. *Proceedings of the Royal Society of London, Ser. A*, Vol. 324, No. 1557, p. 127-55.]
- Weertman, J. 1969. The stress dependence of the secondary creep rate at low stresses. *Journal of Glaciology*, Vol. 8, No. 54, p. 494-95. [Letter.]